Low-cost high-precision PIAA optics for high contrast imaging with exo-planet coronagraphs

Kunjithapatham Balasubramanian,[1a] Stuart B. Shaklan,[a] Laurent Pueyo,[a] Daniel W. Wilson,[a] Olivier Guyon[b]
[a]Jet Propulsion Laboratory, California Institute of Technology
4800 Oak Grove Drive, Pasadena, CA 91109
[b]Steward Observatory, The University of Arizona, Tucson, AZ 85721

ABSTRACT

PIAA optics for high contrast imaging present challenges in manufacturing and testing due to their large surface departures from aspheric profiles at the aperture edges. With smaller form factors and consequent smaller surface deformations (<50 microns), fabrication of these mirrors with diamond turning followed by electron beam lithographic techniques becomes feasible. Though such a design reduces the system throughput to ~ 50%, it still provides good performance down to 2λ/D inner working angle. With new achromatic focal plane mask designs, the system performance can be further improved. We report on the design, expected performance, fabrication challenges, and initial assessment of such novel PIAA optics.

Keywords: PIAA, pupil remapping, high-contrast imaging, coronagraphy, optical fabrication

1. INTRODUCTION

The concept of Phase Induced Amplitude Apodization (PIAA) to suppress diffraction rings and speckles in the image plane of coronagraph for exo-planet imaging was proposed by Olivier Guyon.[1] PIAA coronagraphs test beds at NASA JPL,[2] NASA Ames Research Center[3] and Subaru Telescope[4,5] are currently developing the technology necessary to demonstrate the feasibility of a space coronagraph based on the PIAA concept. Results from these testbeds are very encouraging; but, progress is hampered by the encountered limitations in achieving high performance for various reasons, one of them being the expensive and challenging-to-manufacture PIAA optics. These PIAA systems employ fairly large (~90 mm diameter, in the case of JPL High Contrast Imaging Testbed (HCIT)) mirrors with consequent large mirror sag (~1mm) and large deformation at the outer edges to achieve theoretically high performance at small inner working angles (close to 2λ/D). Our approach is to adopt a conservative design that eases manufacturing complexity and cost with a mild compromise in performance. With an appropriately designed post apodizer and/or a focal plane mask, one can regain the performance of the system. Secondly, fine tuning the profile and surface finish of these mirrors could be accomplished with e-beam lithographic techniques. In conjunction with adaptive optics for wavefront sensing and control to achieve high contrast for imaging planets, such an approach allows a fast technology development for other aspects of the system without imposing undue burden on the PIAA mirrors. With such optics, several labs could attempt to improve the system performance without having to spend >$300K on one component which is the current cost of PIAA mirrors of conventional design and manufacturing. In this paper, we demonstrate the feasibility to fabricate and characterize 1 to 2" diameter high quality PIAA mirrors.

1.1. New Designs

In order to design the low sag PIAA mirrors presented here, we used the following design approach and optimized the surface sag using numerical propagation algorithms to evaluated the broadband contrast of each design.[6] The constraints we imposed on the design are:

- The broadband contrast to be below 10^{-10} for ~20 percent bandwidth at 2λ/D inner working angle (IWA).
- The peak to valley deformation to be below about 50 microns.
- The mirror curvature to be within manufacturing constraints

[1] kbala@jpl.nasa.gov, phone: 1-818-393-0258, fax: 1- 818-393-4950

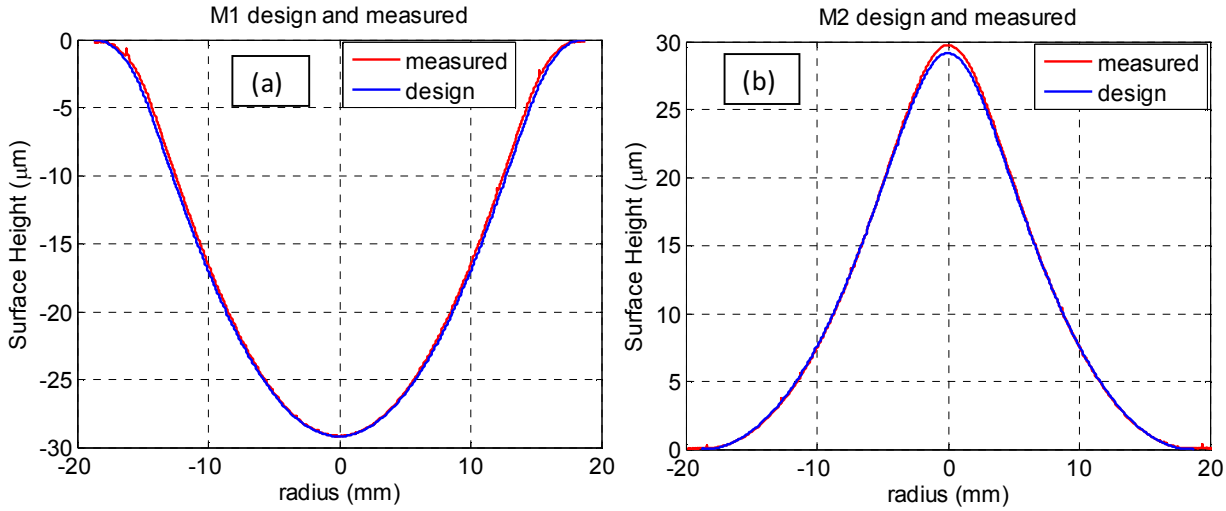

Figure 1 a and b. Design profiles of M1 and M2 mirrors and their measured profiles

The free parameters for the design are:

- The separation z between the mirrors.
- The profile of the pre and post apodizers

The mirror's deformation other than minimal radius of curvature mainly scales as D^2/z and is a weak function of the choice of pre- and post-apodizers. For a given mirror diameter D and mirror separation z, and for the functional form of pre- and post-apodizers chosen for these designs, there is a wide range of apodization parameters that will yield deformations below 50 microns. This means that one can choose ageometry according to the maximal deformation constraint, and then proceed to tuning the apodizers so the broadband contrast constraint is respected. Thus our first step is to satisfy the sag constraint by selecting an adequate geometry, z = 1.6 m for 38 mm diameter optics and z = 1 m for 30 mm. We then proceeded into enforcing the contrast constraint using numerical propagators that evaluate the electric field ringing at M2, which is due to the edge diffraction between M1 and M2. The magnitude of this ringing is the feature that limits the broadband contrast of a given PIAA unit. The purpose of the pre and post-apodizers is to mitigate these chromatic high frequency edge oscillations that are remapped near the center of M2. The amplitude of these remapped Fresnel rings scales as $\lambda.z/ D^2$. Since we chose $\lambda.z/ D^2$ to be about 0.1, 10 times larger than the value corresponding to the reflective PIAA currently under test at HCIT, the apodizers need to be stronger in order to mitigate for larger ringing than in previous generations of PIAA designs. As a consequence, the throughput of our designs is

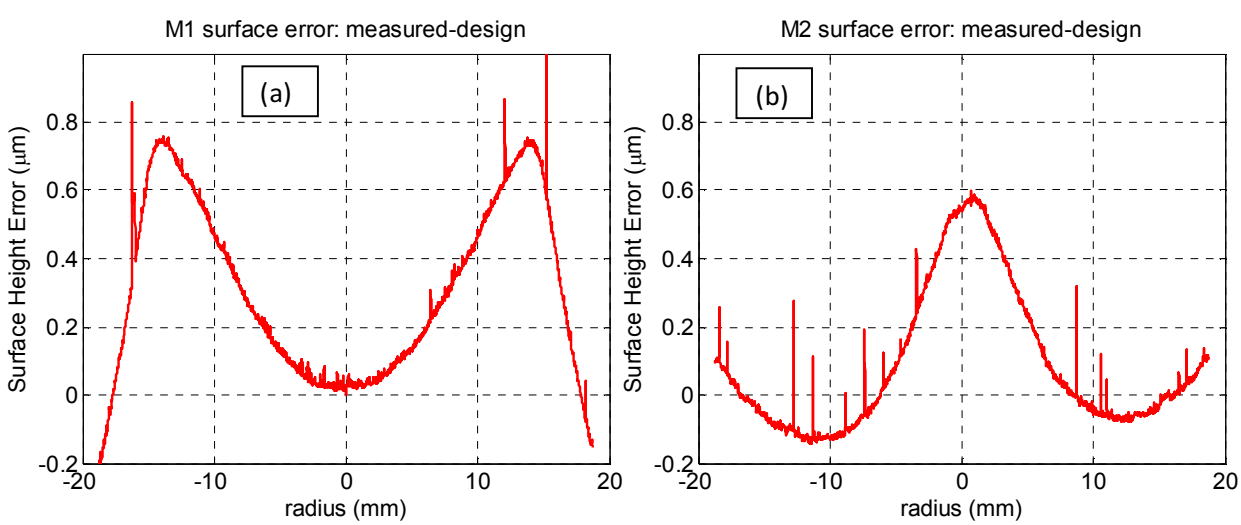

Figure 2 a and b. Profile errors of fabricated Al mirrors M1 and M2 ver1.

limited to 50% and 52% for the 38 mm and 30 mm optics respectively. For the 30 mm optics, the expected IWA contrast is 10^{-9} when implemented with an appropriate post apodizer. To begin with, we designed a pair of 1.5" diameter PIAA mirrors with a sag of ~ 35μm with on-axis parabolic profiles, intended to be used as a pair with a small tilt so that the aberration due to tilt will be small enough and could be compensated by a DM. This pair was designed to provide a contrast of 10^{-10} at the inner working angle of 2λ/D over a 20% bandwidth with ~ 50% throughput. Figure 1 shows the cross-section profiles of these mirrors.

1.2. Fabrication

These first version mirrors were fabricated on 2" diameter aluminum substrates by standard diamond turning techniques. The outer ring regions outside the PIAA diameter were finished to optical quality (<λ/4 finish) so that they could serve as convenient reference surfaces for alignment purposes. Surface profiles of these ver.1 aluminum mirrors measured with a Dektak stylus profilometer are shown in figure 1 along with their design profiles. The deviations from the design profiles are plotted in Figure 2. Note that the error seen is a combination of instrument error plus surface error.

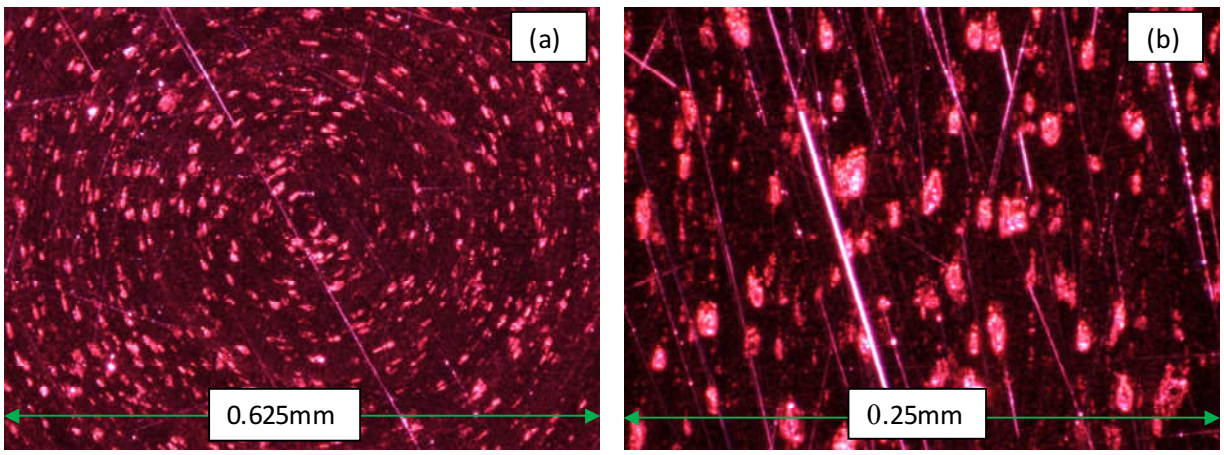

Figure 3. a and b: Surface features of Al mirror M1 due to diamond turning

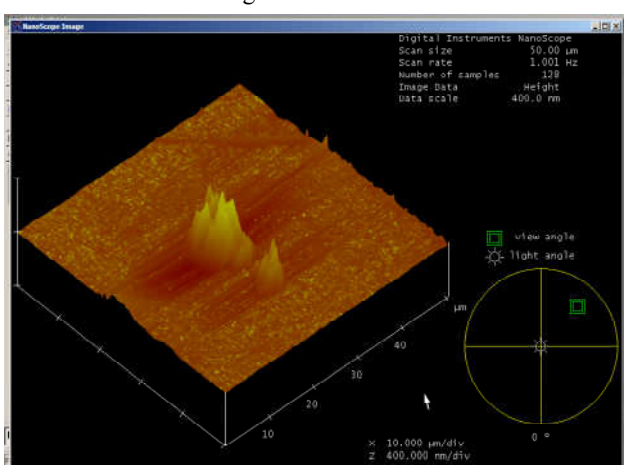

Figure 4. AFM Image of machining mark on Al mirror M1

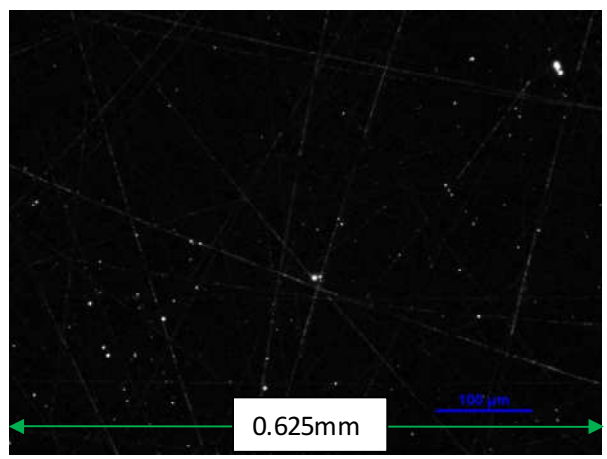

Figure 5. Surface features of OFHC copper mirror M2 due to diamond turning.

2. INSPECTION AND TESTING

2.1. Surface quality

The surface finish of diamond turned mirrors depends on the material used and tools employed. Aluminum mirrors tend to have undesirable surface defects. Figure 3 shows the surface characteristics of the Al mirror M1 in two different

magnifications. AFM image of a machining mark on Al M1 mirror is shown in Figure 4. To assess the material related problems, we designed and fabricated a pair of simple parabolic mirrors of the same dimensions on electronic grade oxygen free high conductivity (OFHC) copper. Significantly better surface finish of copper mirror is shown in Figure 5.

2.2. Wavefront quality

Evaluating wavefront quality of these mirrors is challenging because of their large sag. Steep slopes produce unresolvable fringe density in an interferogram when a plane wavefront is employed. With a Zygo interferometer equipped with a 1kx1k camera, one could observe the fringes in partial sections of the mirrors; by tilting the mirrors, one can obtain interferograms in several radial sections. Figure 6 shows such partial interferograms obtained without tilt. Aligning the mirrors as a pair with the proper separation and minimum tilt as shown in Figure 7 allows one to capture the interferogram over the full diameter after double pass when retroreflected. However, the large mirror separation (1.6m) and air path lead to unstable interferograms. But, with proper enclosures and minimum disturbances, interferograms could be obtained and the wavefront quality of the doublepass beam could be analyzed, though errors may be exaggerated because of the disturbances.

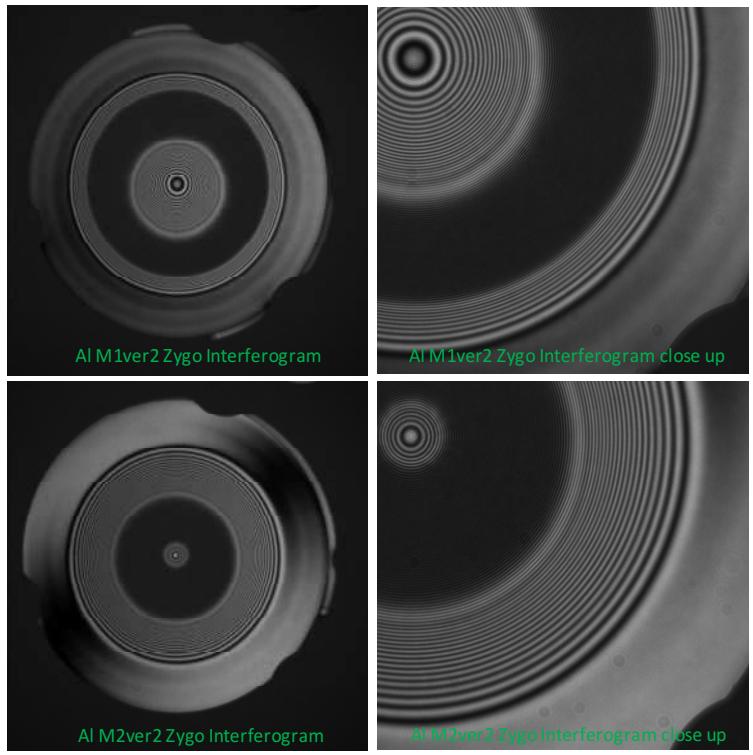

Figure 6. Partial interferograms of M1 and M2.

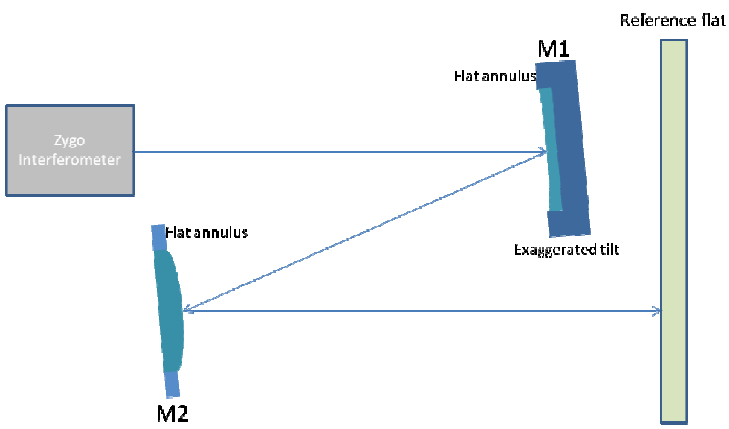

Figure 7. PIAA mirrors M1 and M2 aligned as a pair for wavefront measurement

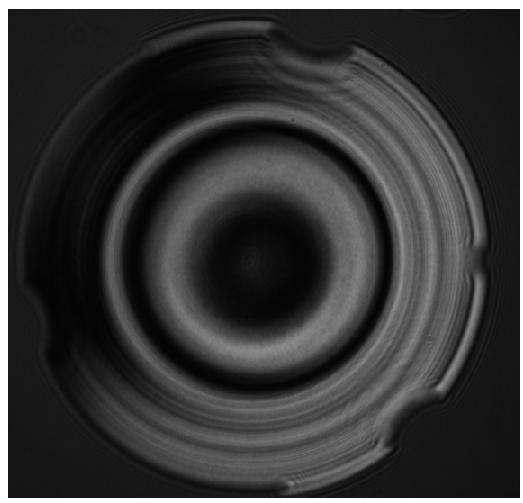

Figure 8. Interferogram of aligned pair of ver2 Al M1 and M2.

Figure 8 shows one such interferogram from an aligned PIAA pair of ver2 (a second set with the same profiles as in Figure 1) of Al M1 and M2. Figure 9 shows the corresponding wavefront analyzed with a Zygo interferometer. With less than 0.1wv r.m.s wavefront error and with scope for better alignment, these mirrors are seen to be of high quality except for the residual power which can be compensated by defocus.

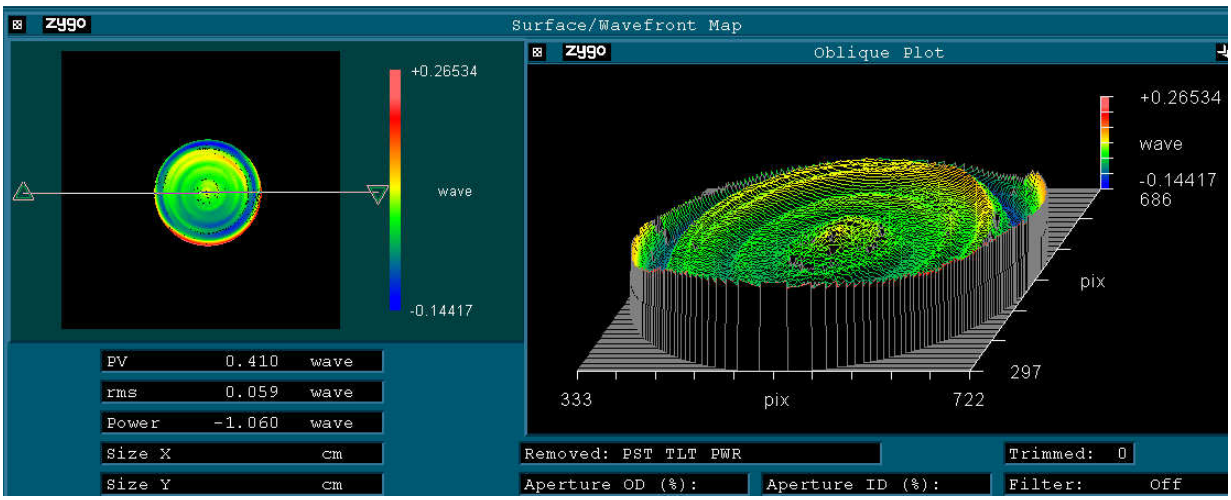

Figure 9. Wavefront map of aligned pair of Al M1 and M2 (ver2) showing less than 0.1wave r.m.s. wavefront error

FINE TUNING THE MIRROR SURFACE BY E-BEAM LITHOGRAPHY

Small curvature error and other localized surface defects due to diamond turning potentially could be corrected by analog-relief electron-beam lithographic techniques that have been successfully used to fabricate blazed gratings on convex and concave substrates.[7]

To examine the accuracies achievable by this technique, one of the ver1 Al mirrors was resurfaced with a polymer on two zones as shown in Figure 10. The bare mirror profile is shown in the lower curve. The mirror was uniformly coated with several microns of polymer, then this was lithographically processed to attain the 'notches' and roll off the wavefront at the edge of the surface as shown in the upper curves. The goal was to determine the surface accuracy and limiting errors due to the lithographic process. A profile of the resurfaced mirror measured by a Dektak stylus profilometer is shown in Figure 11. Agreement is fairly good, but surface roughness is evident. As seen in Figure 12, an AFM image of the refinished zone shows e-beam stitching errors of 50 to 200 nm in height due to errors in the e-beam deflector calibration. Both field boundaries (~500 µm spacing) and subfield boundaries (~4 µm spacing) are evident. It might be possible to nearly eliminate the subfield boundaries with better calibration, but some level of field boundaries will always be present due to exposure of the non-flat surface. Hence surface roughness may ultimately limit the utility of this technique.

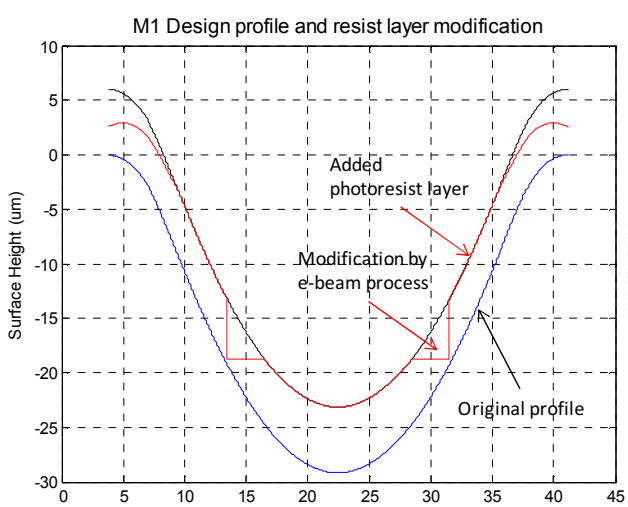

Figure 10. E-beam lithographic modification of surface profile and finish. The x-axis of the plot is mm.

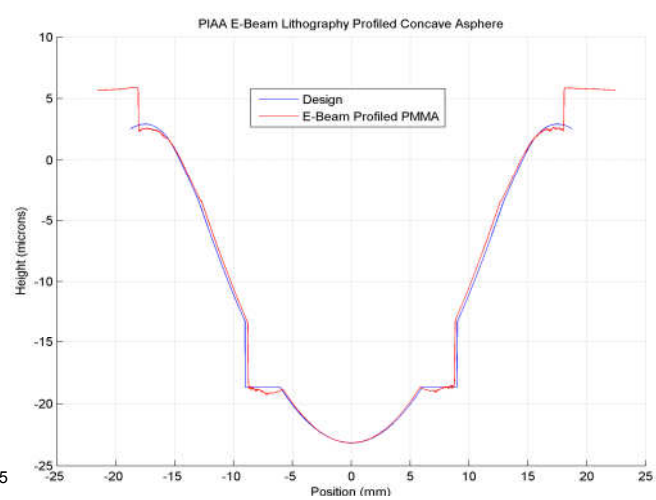

Figure 11 Comparison of the measured E-beam profiled surface with the design.

3. Ni ON SUPER-INVAR

Considering the unfavorable thermal properties of aluminum and copper, electroless Nickel plated SuperInvar[8] with 10x smaller thermal expansion coefficient was considered favorable to study the feasibility. Hence, a pair of Ni/Super Invar mirrors was fabricated by diamond turning. For this pair, a diameter of 30 mm was chosen to match the beam dimensions in HCIT to enable potential coronagraph testing later. These mirrors have very few pits/bumps due to diamond turning though grooves are clearly observable as shown in Figure 13. These shallow grooves can be smoothened by applying a layer of PMMA overcoated with aluminum. The surface can be further tuned by e-beam lithography. The fully assembled pair of these Ni/Invar mirrors without any further surface polish shows very good wavefront quality in double pass measurement with a Zygo interferometer as shown in Figures 14 and 15. The residual errors found are correctable with better alignment and an adaptive wavefront control system.

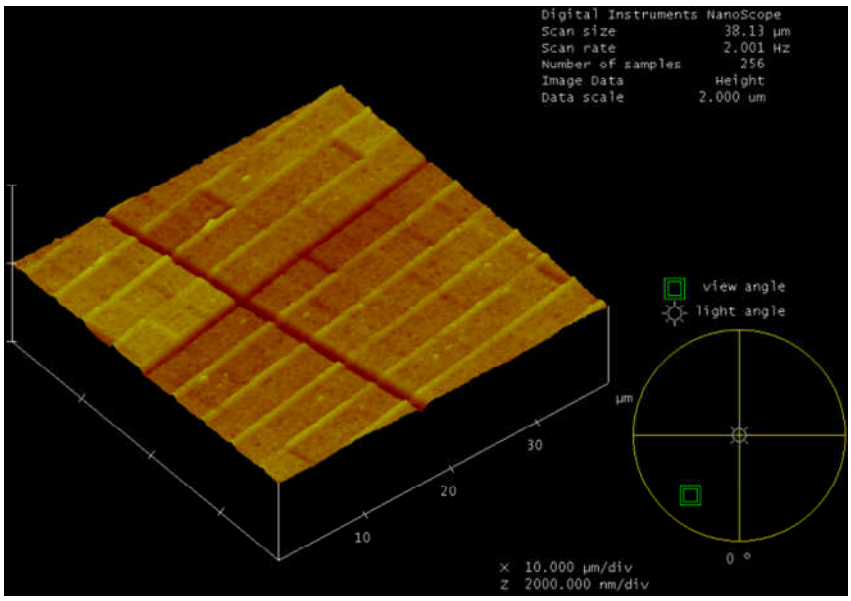

Figure 12. Atomic force microscope scan of the E-beam profiled surface. Stitching errors of the field (large) and subfield (small) e-beam deflection systems are seen.

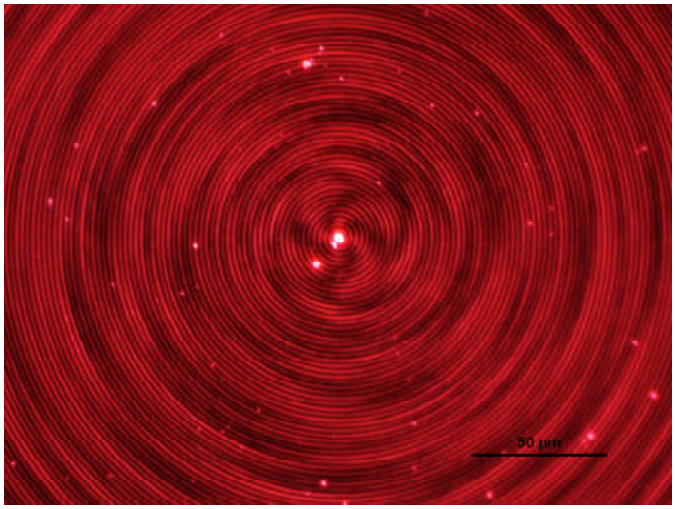

Figure 13. Surface features of Ni/Super Invar mirror M2

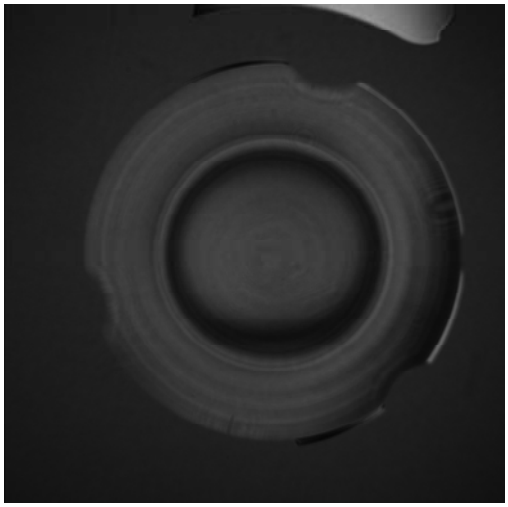

Figure14. Double pass wavefront interferogram of 30 mm diameter Ni/Super Invar mirror pair

4. CONCLUSIONS

The results obtained from this preliminary study clearly demonstrate the feasibility to manufacture high quality PIAA mirrors with acceptable performance at a fraction of the cost of manufacturing them by other methods. The next step is to test them in a coronagraph testbed with a deformable mirror to assess the limiting contrast achievable with such mirrors. Theoretical simulations show that a contrast of 10^{-10} at the inner working angle of $2\lambda/D$ over a 20% bandwidth

with ~ 50% throughput can be obtained when appropriately designed pre- and post-apodizers are employed. As the cost and turn-around time of these mirrors is significantly smaller than others, one can design and manufacture several versions of potential systems for testing in various labs so that fast progress of technology development on other aspects of the system to higher TRL levels can be accomplished at relatively low cost.

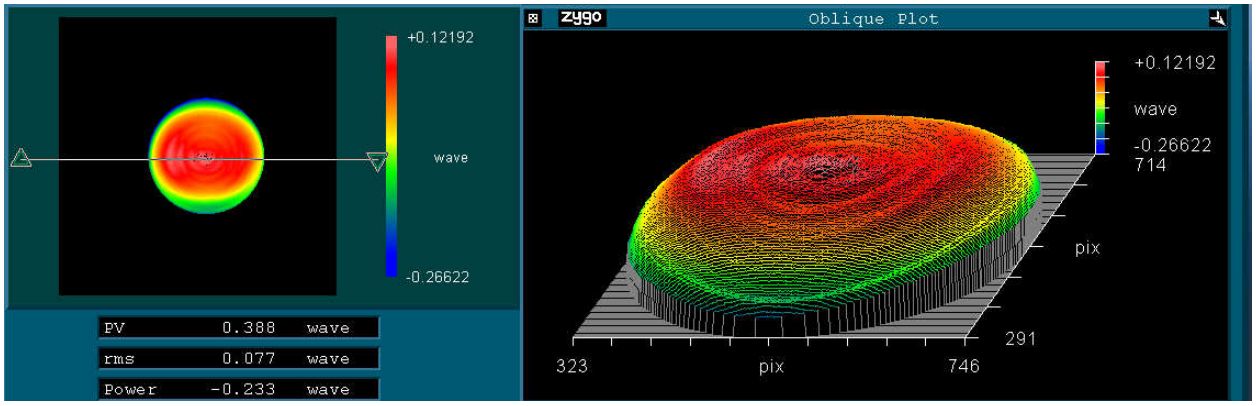

Figure 15. Doublepass wavefront map of 30 mm diameter Ni/Super Invar mirror pair

5. ACKNOWLEDGEMENTS

The authors gratefully acknowledge the valuable discussions with Dr. Ruslan Belikov and Dr. Eugene Pluzhnik, both of NASA Ames Research Center (ARC) and their help with initial evaluation of the first set of these mirrors in their lab at ARC. This work was carried out at the Jet Propulsion Laboratory, California Institute of Technology, under contract to the National Aeronautics and Space Administration.

6. REFERENCES

[1] Guyon, O., “Phase-induced amplitude apodization of telescope pupils for extrasolar terrestrial planet imaging," Astronomy and Astrophysics 404, 379-387 (June 2003).
[2] Kern, B., “Phase-induced amplitude apodization (PIAA) coronagraph testing at the High Contrast Imaging Testbed.,” Proceedings of SPIE Vol. 7440, 74400H (2009).
[3] Belikov, R., “First results on a new PIAA coronagraph testbed at NASA Ames,” Proceedings of SPIE Vol. 7440, 74400J (2009).
[4] Guyon O., *et al,* "High Contrast Imaging and Wavefront Control with a PIAA Coronagraph: Laboratory System Validation," Publ. Astron. Soc. Pacific, 122, 71-84 (2010).
[5] Guyon, O.,"Exoplanet Imaging with a Phase-induced Amplitude Apodization Coronagraph. I. Principle" . ApJ 622 , 744 (2005).
[6] Pueyo, L.,“Numerical propagator through PIAA optics, ” Proceedings of SPIE Vol. 7440, 74400E (2009).
[7] Wilson., D. W., “Electron-beam lithography for micro and nano-optical applications” Proceedings of SPIE Vol. 5720, 68 (2005).
[8] Meinel, A. M., “Wavefront correctors by diamond turning,” Applied Optics, 25, 824-825 (1986).